Letter

Phase versus coin versus position disorder as a probe for the resilience and revival of single-particle entanglement in cyclic quantum walks

Dinesh Kumar Panda [*] and Colin Benjamin [†]

School of Physical Sciences, National Institute of Science Education and Research Bhubaneswar, Jatni 752050, India and Homi Bhabha National Institute, Training School Complex, Anushaktinagar, Mumbai 400094, India

(Received 18 October 2024; revised 28 January 2025; accepted 2 April 2025; published 16 April 2025)

Quantum states exhibiting single-particle entanglement (SPE) can encode and process quantum information more robustly than their multiparticle analogs. Understanding the vulnerability and resilience of SPE to disorder is therefore crucial. This letter investigates phase, coin, and position disorder via discrete-time quantum walks on odd and even cyclic graphs to study their effect on SPE. The reduction in SPE is insignificant for low levels of phase or coin disorder, showing the resilience of SPE to minor perturbations. However, SPE is seen to be more vulnerable to position disorder. We analytically prove that maximally entangled single-particle states (MESPS) at time step $t = 1$ are impervious to phase disorder regardless of the choice of the initial state. Further, MESPS at timestep $t = 1$ is also wholly immune to coin disorder for phase-symmetric initial states. Position disorder breaks odd-even parity and distorts the physical time cone of the quantum walker, unlike phase or coin disorder. SPE saturates toward a fixed value for position disorder, irrespective of the disorder strength at large timestep t. Furthermore, SPE can be enhanced with moderate to significant phase or coin disorder strengths at specific time steps. Interestingly, disorder can revive single-particle entanglement from absolute zero in some instances, too. These results are crucial in understanding single-particle entanglement evolution and dynamics in a laboratory setting.

DOI: 10.1103/PhysRevE.111.L042103

Introduction. Single-particle entanglement or SPE refers to entanglement between different degrees of freedom (DoF) of a single particle such as a laser-cooled ion trap or a photon [1–5]. Quantum states exhibiting SPE can encode more extensive quantum information (QI) than their multiparticle analogs exploiting large Hilbert space [6]. These SPE states are more robust to decoherence and advantageous for quantum communication and cryptography [2,4,7]. Further, these have applications in large-scale QI processing, quantum state exploration, and studying the interaction between fundamental particles [2,8–12]. However, these are challenging to generate and control. Such states with large or maximal SPE can be generated efficiently via discrete-time quantum walks (DTQWs) [3,4,7,13–15]. Note that DTQWs have experimental realization using lattice-based quantum systems whose position space matches the discrete lattice sites, such as cold atoms [16,17], photons [18–22], trapped ion [23,24], and NMR system [25].

In a recent letter, we found recurrent generation of maximally entangled single-particle states (MESPS or maximal SPE states) via a single coin in cyclic DTQW (without disorder), see Ref. [4]. However, how such MESPS (i.e., a state with maximal SPE) or an SPE state would behave in the presence of disorder is yet to be studied. In addition, whether a disorder can revive SPE is a fundamental research question. Such a study is paramount as disorder/noise is ubiquitous and sometimes unavoidable in quantum systems. We bridge this fundamental research gap and comprehensively investigate the effects of phase, coin, and position disorder (of arbitrary strengths) on DTQW dynamics in odd or even cyclic graphs and the generated position-coin (quNit-qubit) SPE states.

In a cyclic DTQW (CQW) without disorder (i.e., clean-CQW), one can generate MESPS for arbitrary initial states under certain conditions. We showed this in Ref. [4], and with a Hadamard coin operator, one generates recurrent MESPS with period four at time steps $t = 1, 5, 9, ...$, via the clean-CQW for an arbitrary initial state, see [4]. In this Letter, we find that the reduction in SPE is insignificant for low levels of phase or coin disorder, showing the resilience of SPE to minor disturbances. SPE is, however, more vulnerable to position disorder. For phase disorder, MESPS (maximal SPE state) at time step $t = 1$ remains unperturbed for any arbitrary initial state. For coin disorder, however, only two specific phase-symmetric initial states give foolproof immunity against disorder for MESPS at $t = 1$. Position disorder breaks odd-even parity [26] [i.e., position $x = 0$ probability: $P(x = 0) \neq 0$ at odd t] and distorts the physical time cone of the quantum walker, unlike phase or coin disorder. SPE saturates towards a fixed value for position disorder, irrespective of the disorder strength, for more significant time steps.

Further, SPE can be enhanced with moderate or more significant phase or coin disorder strength at specific time steps. Notably, disorder can also revive single-particle entanglement. One can tune the SPE value by controlling the strength of various disorders [27], and this work aligns with laboratory implementations [18–22] for quantum systems evolving via

[*]Contact author: dineshkumar.quantum@gmail.com
[†]Contact author: colin.nano@gmail.com

 ©2025 American Physical Society

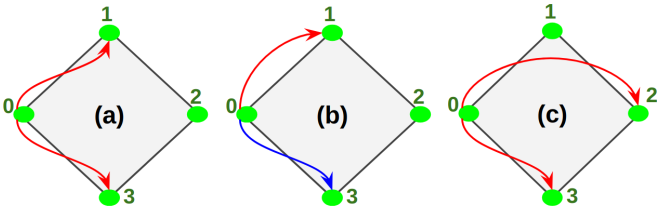

FIG. 1. (a) Clean CQW; (b) CQW with phase or coin disorder, where amplitudes in coin basis change; (c) CQW with position disorder where jump length in shift changes randomly. Sites are shown as green dots, and red (for the same amplitudes) and blue (for different amplitudes) curves denote amplitudes of the particle on fourcycle.

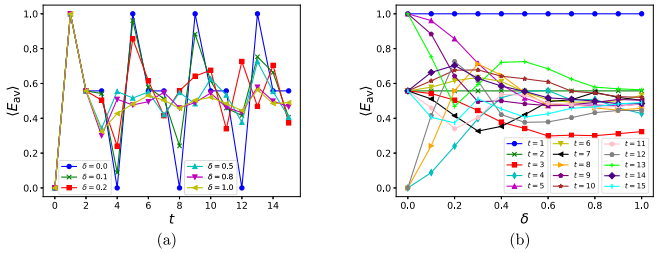

FIG. 2. (a) SPE $\langle E_{\rm av}\rangle$ vs time step t for different static-phase-disorder strengths (δ); (b) SPE $\langle E_{\rm av}\rangle$ vs static-phase-disorder strength δ for different t for four cycle.

CQWs. This counterintuitive result of enhancement, revival, and resilience of SPE is a byproduct of the interplay between disorder, interference, and unitary quantum evolution [28–31]. This motivates strategies to harness noise/disorder for enhancing entanglement, safeguarding quantum coherence, and exploring quantum error mitigation (which is reliant on precise noise characterization) techniques for large-scale QI processing and quantum computation [31–34].

Below, we present a generalized CQW model (with and without the disorder) for odd- and even-site cyclic graphs that beget a rich class of quantum states and generate SPE between the walker's position-coin DoF. Then, we discuss the behavior of generated SPE (from clean CQW dynamics) under phase disorder, coin disorder, and position disorder of arbitrary strengths. After that, we analyze the disorder effects on the generated SPE states, compare our results with other relevant approaches, and finally draw conclusions from this comprehensive study. Additional details on generalized disordered CQW dynamics, its properties, and SPE vs disorder for both four and three cycles are provided in the Supplemental Material (SM) [35].

CQW and single particle entanglement. A quantum particle evolving via DTQW dynamics on a k-site cyclic graph (k cycle, see Fig. 1) is defined on a Hilbert space ($\mathcal{H}$), combining its k-dimensional position ($\mathcal{H}_P$) and two-dimensional coin ($\mathcal{H}_C$) spaces. $\mathcal{H}_C$ and $\mathcal{H}_P$ are spanned by computational bases $\{|0_c\rangle, |1_c\rangle\}$ and $\{|x_p\rangle : x \in 0, 1, 2, \ldots, k-1\}$, respectively, and $\mathcal{H} = \mathcal{H}_P \otimes \mathcal{H}_C$. A physical quantum walker is a photon (or a cold-trapped ion) wherein $\mathcal{H}_C$ and $\mathcal{H}_P$ correspond to its polarization (hyperfine electronic states) and path (local position) DoF, respectively [1,17,18,27]. When the quantum walker (particle) is initially localized at site $|0_p\rangle$ in an arbitrary superposition of coin states $|q_c\rangle$, its initial state, $|\psi(t=0)\rangle$ reads

$$|\psi(t=0)\rangle = |0_p\rangle \otimes \left[\cos\left(\frac{\theta}{2}\right)|0_c\rangle + e^{i\phi}\sin\left(\frac{\theta}{2}\right)|1_c\rangle\right], \tag{1}$$

where $\theta \in [0, \pi]$ and $\phi \in [0, 2\pi)$. The quantum walker evolves unitarily via a time-dependent evolution operator $U_k(t)$ and after t time steps, is in the evolved state

$$\begin{aligned}|\psi(t)\rangle &= U_k(t)U_k(t-1)...U_k(1)|\psi(t=0)\rangle, \\ &= \sum_{x=0}^{k-1}[\alpha_0(x,t)|x_p, 0_c\rangle + \alpha_1(x,t)|x_p, 1_c\rangle],\end{aligned} \tag{2}$$

where the amplitudes $\alpha_0(x,t)$ and $\alpha_1(x,t)$ depend on initial state [Eq. (1)] and the design of the evolution operator, $U_k(t) = \hat{S}(t) \cdot [\sum_x |x_p\rangle\langle x_p| \otimes \hat{C}(\rho(x,t))]$.

We use a general qubit-coin operator,

$$\hat{C}(\rho) = \begin{pmatrix} \sqrt{\rho} & \sqrt{1-\rho} \\ \sqrt{1-\rho} & -\sqrt{\rho} \end{pmatrix}, \quad \text{with } 0 \leqslant \rho \leqslant 1, \tag{3}$$

to introduce arbitrary superposition in the walker's coin subsystem. Subsequently, a shift operator $\hat{S}(t)$ is employed to move the walker to the left (right) in the position basis by hopping (jump) length $J(t)$ which is contingent on the coin state $|0_c\rangle$ ($|1_c\rangle$). The typical translation (or shift) operator reads

$$\hat{S}(t) = \sum_{s=0}^{1}\sum_{x=0}^{k-1}|((x+2s-J(t)) \bmod k)_p\rangle\langle x_p| \otimes |s_c\rangle\langle s_c|. \tag{4}$$

To obtain the well-known Hadamard walk in a k cycle, one sets $\rho = \frac{1}{2}$ [i.e., Hadamard coin $\hat{H} = \hat{C}(\frac{1}{2})$] and $J(t) = 1, \forall t$, see also Ref. [4]. We observe for the Hadamard coin CQW and any arbitrary general initial state Eq. (1), which is clean CQW (i.e., without disorder), for the following three fundamental properties:

(i) It preserves the odd-even parity [26] only for even k-cycle graphs like four cycle, i.e., at even (odd) t, only even (odd)-numbered sites have finite probabilities of walker's occupation. For details, see Sec. A in the SM [35]. Physically, this implies a photon (a walker) can not be found at even sites once it has evolved to an odd t.

(ii) It respects the physical time cone of the walker for all k cycle, i.e., a walker found at position $|x_p\rangle = |m_p\rangle$ for time step t, will have finite probability of being found at positions up to $|x'_p\rangle = |((m \pm n) \bmod k)_p\rangle$ at time step $(t+n)$. For details, see Sec. A in the SM [35].

(iii) It generates MESPS at time step $t = 1$ for any arbitrary k-cycle graph. Corollary: for four and eight cycles, MESPS is generated recurrently with period four at time step $t = 1, 5, 9, ...$, see Fig. 2(a) (blue), see also [4]. The generic time evolution of CQW dynamics with general initial state Eq. (1) for arbitrary qubit coin [Eq. (3)] and general translation operator [Eq. (4)], which generates high-dimensional (quNit-qubit) single particle entanglement between the position (quNit, $N = k$) and the coin (qubit) DoF of the walker, is detailed in Sec. A in the SM [35].

In order to quantify the amount of quNit-qubit entanglement (SPE) in the disordered CQW, we employ entanglement

entropy (E) [4,27,36]. E at any t is defined as the von-Neumann entropy of the reduced density matrix $\rho_c(t) = \mathrm{Tr}_p(|\psi(t)\rangle\langle\psi(t)|)$, i.e., $E(\rho_c) = -\mathrm{Tr}(\rho_c \log_2 \rho_c)$. If E_0 and E_1 are the eigenvalues of $\rho_c(t)$, one equivalently estimates $E = -\sum_{s=0}^{1} E_s \log_2 E_s$. The average SPE is then, $E_{\mathrm{av}} = \frac{1}{\pi}\int_0^{\pi} E\, d\theta$ for $\phi = \frac{\pi}{2}$ and SPE states are guaranteed for $0 < E_{\mathrm{av}} \leqslant 1$. For separable states like the initial state (1), $E_{\mathrm{av}} = 0$, and for the state evolving via a clean CQW at $t = 1$ [see Sec. A in the SM [35] and Eq. (2) with Hadamard coin], we see $E_{\mathrm{av}} = 1$, i.e., it is a MESPS.

Phase disorder and SPE in CQW. Phase disorder in the CQW setup can be site dependent (static) or time dependent (dynamic). Below, we first investigate the effect of static and then the dynamic phase disorder on CQW evolution and generated SPE.

Static-phase disorder. The static-phase disorder is introduced in the CQW setup through the following translation operator [modified Eq. (4) without time-dependence], i.e.,

$$\hat{S}_{sp} = \sum_{s=0}^{1}\sum_{x=0}^{k-1} |((x+2s-1) \bmod k)_p\rangle\langle x|\, e^{i\alpha_s(x)} \otimes |s_c\rangle\langle s_c|, \tag{5}$$

where $\alpha_s(x)$ with $s \in \{0, 1\}$ are site-dependent phase angles. Any CQW property will only depend on the fluctuations in relative phase difference $\alpha_0(x) - \alpha_1(x)$, as we can factor out the phase $e^{i\alpha_1(x)}$ (while estimating a physical observable), i.e., $\hat{S}_{sp} = \sum_{x=0}^{k-1} e^{i\alpha_1(x)}(|((x-1) \bmod k)_p\rangle\langle x|\, e^{i(\alpha_0(x)-\alpha_1(x))} \otimes |0_c\rangle\langle 0_c| + |((x+1) \bmod k)_p\rangle\langle x| \otimes |1_c\rangle\langle 1_c|)$. Thus, randomizing the phase angle $\alpha_0(x)$ only, i.e., by choosing it randomly from the set $[0, \delta]$ in units of π with a uniform distribution [37], and keeping $\alpha_1(x) = 0$ (constant), introduces a finite random phase difference, i.e., a generalized phase disorder in the CQW setup. The probability density function for a uniform distribution reads

$$f(\alpha_0(x)) = \frac{1}{b-a} \quad \text{for real} \quad a \leqslant \alpha_0(x) \leqslant b. \tag{6}$$

Here, $a = 0, b = \delta$ and the full CQW evolution is then, $U_k(t) = \hat{S}_{sp} \cdot [\sum_x |x\rangle\langle x| \otimes \hat{H}]$. Clearly, at $\delta = 0$, we retrieve the clean-CQW. Thus, $|\psi(t)\rangle = \hat{S}_{sp} \cdot [\sum_x |x\rangle\langle x| \otimes \hat{H}]|\psi(t-1)\rangle$.

In the numerical simulation of the static-phase disorder case, a set of random on-site phase $\alpha_0(x)$ values is generated, with its size corresponding to the maximum spread of the walker for up to a specific time step (say, $t = 15$). This site-dependent set remains constant throughout the specified time steps, representing one disorder realization. In our study, any CQW measure $\Omega_1(t)$, such as the entanglement entropy (E_{av}) or the walker's position probability [$P_{\mathrm{av}}(x = 0)$], is first evaluated for a specific disorder realization. In this study, 500 such disorder realizations are computed to estimate the realization-average (quenched average, as one random-phase set is fixed to a particular realization) [26], $\langle\Omega_1(t)\rangle$, i.e., $\langle\Omega_1(t)\rangle = \frac{1}{500}\sum_{j=1}^{500} \Omega_1(|\psi(t)\rangle_j\langle\psi(t)|_j)$. Static phase disorder does not affect the hopping length [i.e., $J(t) = 1, \forall t$] nor the qubit coin, $\hat{H}$. Thus, the odd-even parity is preserved as in the clean-CQW case for four cycle. It is shown in Fig. 2(a) of SM [35], where we see the probability of finding the walker $\langle P_{\mathrm{av}}(x = 0)\rangle$ at odd time steps is always zero. Phase disorder also does not hinder the walker's physical time cone for the same reason as also seen for the clean CQW.

Interestingly, SPE dynamics shows significant differences under static phase disorder for different disorder strengths, i.e., for δ ranging from 0 (clean CQW) to 1 in units of π, see Fig. 2 for four cycle. From Figs. 2(a), 2(b), and the SM [35], for odd three cycle, we observe that MESPS, at $t = 1$, is robust against static phase disorder of any arbitrary strength. To prove this robustness, we find the time-evolved state, with Eq. (1) for $\phi = \frac{\pi}{2}$,

$$|\psi(t=1)\rangle = \hat{S}_{sp} \cdot \left[\sum_x |x\rangle\langle x| \otimes \hat{H}\right] \times \frac{\cos\left(\frac{\theta}{2}\right)|0_p, 0_c\rangle + i\sin\left(\frac{\theta}{2}\right)|0_p, 1_c\rangle}{\sqrt{2}}. \tag{7}$$

Using Eq. (5), one obtains from Eq. (7),

$$|\psi(t=1)\rangle = \frac{1}{\sqrt{2}}\Bigg[\left(\cos\left(\frac{\theta}{2}\right) + i\sin\left(\frac{\theta}{2}\right)\right) \times e^{i\alpha_0(0)}|(k-1)_p, 0_c\rangle + \left(\cos\left(\frac{\theta}{2}\right) - i\sin\left(\frac{\theta}{2}\right)\right)|1_p, 0_c\rangle\Bigg], \tag{8}$$

and from its density matrix $|\psi(t=1)\rangle\langle\psi(t=1)|$, we get the reduced density matrix, $\rho_c(t=1) = \mathrm{Tr}_p(|\psi(1)\rangle\langle\psi(1)|)$, i.e., $\rho_c(t=1) = \frac{1}{2}\begin{pmatrix}1 & 0\\ 0 & 1\end{pmatrix}$, which is maximally mixed independent of the choice of initial state parameter θ, random phase angles $\alpha_0(0)$, and the number of sites (k) in the cyclic graph. The entanglement entropy of this state is

$$E(\rho_c) = -\mathrm{Tr}(\rho_c \log_2 \rho_c) = \tfrac{1}{2}\log_2(2) + \tfrac{1}{2}\log_2(2) = 1, \tag{9}$$

which proves the state in Eq. (8) has maximal SPE and is a MESPS (a single-particle Bell state). The MESPS at $t = 1$ is robust against static phase disorder of arbitrary strength and for any initial state, i.e., for an infinite number of initial states [Eq. (1)] with arbitrary θ; also see Fig. 2(b). The recurrence or periodicity of SPE via four-cycle CQW is lost for phase disorder, and no recurrence occurs for three cycle under such disorder, i.e., it remains chaotic even under such disorder, also see Fig. 3 in the SM [35]. From Fig. 2(b), one can observe that SPE remains almost unaffected by small disorder strengths δ; see, for example, SPE values at $t = 3, 5, 7, \ldots$. These results are valid for small time steps ($t \leqslant 8$), see Figs. 2(a) and 2(b); for larger t, SPE is vulnerable to all disorder strengths due to the strong coupling between the evolved state and disorder, i.e., the disorder effect piles up in course of time and at large t, disorder effects on SPE can be quite significant. Further, SPE increases under the phase disorder too, see for example SPE values at $t = 6, 10, 14, \ldots$, in Figs. 2(a) and 2(b). In addition, we observe that the static phase disorder can revive single-particle entanglement from zero, i.e., from an otherwise separable state observed at $t = 4, 8, 12$, see Fig. 2(b) (cyan, yellow, and gray) and Fig. 2(a) (blue). We find similar results for the three-cycle case, see the SM [35] (Fig. 3), i.e., SPE can increase or decrease for static phase disorder of appropriate strength. Moreover, at $t = 1$, MESPS is resilient to static phase disorder and initial state choice, as seen in the four-cycle case.

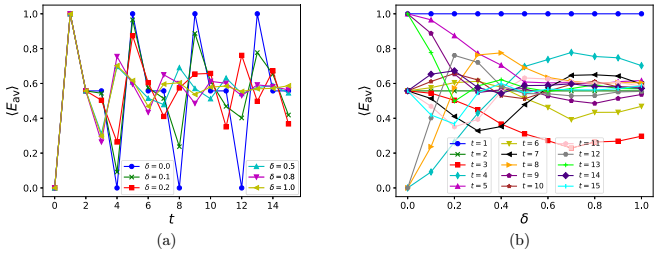

FIG. 3. (a) SPE $\langle E_{\rm av}\rangle$ vs time step t for different dynamic-phase-disorder strength (δ); (b) SPE $\langle E_{\rm av}\rangle$ vs dynamic-phase-disorder strength δ for different t for four cycle.

Dynamic-phase disorder. The dynamic-phase disorder can be introduced in the CQW setup through the following translation operator [from Eq. (4)], i.e., $\hat{S}_{dp}(t) = \sum_{s=0}^{1}\sum_{x=0}^{k-1} |((x+2s-1) \bmod k)_p\rangle\langle x| \, e^{i\beta_s(t)} \otimes |s_c\rangle\langle s_c|$, where the time-dependent relative phase angles $\beta_0(t)$ [with keeping $\beta_1(t) = 0$, for the similar reason discussed below Eq. (5)] are random numbers $[0, \delta]$ in units of π drawn from uniform distribution, i.e., Eq. (6) with $\beta_0(t)$ in the place of $\alpha_0(x)$. The full CQW evolution is now $U_k(t) = \hat{S}_{dp}(t) \cdot [\sum_x |x\rangle\langle x| \otimes \hat{H}]$ [which is different from $U_k(t)$ for static-phase disorder]. Finally,

$$|\psi(t)\rangle = \hat{S}_{dp}(t) \cdot [\sum_x |x\rangle\langle x| \otimes \hat{H}]|\psi(t-1)\rangle. \tag{10}$$

In the numerical simulation of the dynamic disorder, unlike the static-phase case, a set of time-dependent (and site-independent) random phase $\beta_0(t)$ angles is generated, with its length equal to the maximum time steps considered for the CQW dynamics (say, $t = 15$). It represents one disorder realization, and subsequently, a realization average is computed with 500 such realizations for any quantity $\Omega_2(t)$, such as $E_{\rm av}$ or $P_{\rm av}(x = 0)$, i.e., $\langle\Omega_2(t)\rangle = \frac{1}{500}\sum_{j=1}^{500} \Omega_2(|\psi(t)\rangle_j\langle\psi(t)|_j)$. A dynamic phase disorder preserves both the odd-even parity for a four cycle and the particle's physical time cone for all cycles, as also seen for the static variant; see Fig. 2 in the SM [35].

Interestingly, the SPE dynamics shows remarkable divergence under the dynamic-phase disorder of different strengths, i.e., for δ ranging from 0 (clean-CQW) to 1 in units of π, see Fig. 3, and the SM [35]. SPE (MESPS) recurrence via four-cycle CQW is lost for dynamic phase disorder, and no recurrence occurs for three cycle. From Figs. 3(a) and 3(b), we observe that MESPS, at $t = 1$, is robust against dynamic phase disorder of arbitrary strength too, i.e., it gives a Bell (MESPS) state irrespective of the phase disorder strength, also see Sec. B in the SM [35] for its detailed proof. This result holds for any initial state, see Eq. (1), and for any arbitrary θ (with $\phi = \frac{\pi}{2}$). From Fig. 3(b), one can observe that SPE is almost unaffected for small disorder strengths δ, see SPE values at $t = 3, 5, 7, ...$, and SPE increases due to dynamic-phase disorder, see SPE values at $t = 4, 6, 8, 10, 12, 14, ...$ In addition, we observe that the dynamic phase disorder revives single-particle entanglement from zero, i.e., from an otherwise separable state, see Fig. 3(a) (blue) and Fig. 3(b) (cyan, yellow, gray) at $t = 4, 8, 12$. We find similar results for the three-cycle case, see Fig. 4 in the SM [35], i.e., SPE can increase and decrease due to dynamic phase disorder. Moreover, for the three cycle, at $t = 1$, MESPS is resilient to dynamic-phase disorder and initial state choice, as also seen for the four-cycle case, see Sec. B in the SM [35].

Static vs dynamic phase disorder. Although static and dynamic phase disorders have similar effects on the CQW and generated SPE values, like preserving odd-even parity (four cycle), obeying physical time cone, and increasing SPE, as well as reviving SPE from zero, static-phase disorder, on average, is the stronger phase disorder, see SPE values at $t = 4, 8, 12, 15$ in Figs. 2 and 3. There, we see that static phase disorder reduces SPE more than the dynamic variant.

Coin disorder and SPE in CQW. Coin disorder in CQW setup can also be site dependent (static) or time dependent (dynamic). The former is introduced in the CQW setup through modified evolution, i.e., $U_k(t) = \hat{S}(t) \cdot [\sum_x |x\rangle\langle x| \otimes \hat{C}(\rho(x))]$ with site-dependent coin operators [26] and the latter via $U_k(t) = \hat{S}(t) \cdot [\mathbf{I}_P \otimes \hat{C}(\rho(t))]$, with time-dependent coin operators. For both static and dynamic coin disorder of strength (ω), translation operator is $\hat{S}(t)$ [see, Eq. (4)], with hopping length $J(t) = 1, \forall t$, and MESPS at $t = 1$ remains unperturbed for both three and four cycles, for two phase-symmetric initial states, i.e., $\frac{|0_p,0_c\rangle \pm i|0_p,1_c\rangle}{\sqrt{2}}$, see Eq. (1) with $\theta = \frac{\pi}{2}$ with $\phi = \frac{\pi}{2}, \frac{3\pi}{2}$. See Sec. C in the SM [35] for its complete analytical derivation and more details. Therein, we also observe that SPE remains almost unaffected by low levels of coin disorder. The static and dynamic coin disorders can also increase SPE at specific time steps. In addition, we observe that both the static and dynamic coin disorders revive SPE from zero, i.e., from an otherwise separable state observed at $t = 4, 8, 12$, see Sec. C in the SM [35] and Fig. 5(b). Static and dynamic coin disorder have many similar effects on CQW and generated SPE values, such as both preserving odd-even parity (four cycle), obeying physical timecone (all cycles), increasing SPE (at specific time steps t), as well as reviving SPE from zero. However, static coin disorder, on average, is the more substantial coin disorder, see Sec. C in the SM [35] and Figs. 5–8, where we see the static coin disorder reduces SPE more than the dynamic variant for both three and four cycles.

Position disorder and SPE in CQW. Position disorder can be introduced in CQW dynamics via the evolution, $U_k(t) = \hat{S}(t) \cdot [\mathbf{I}_P \otimes \hat{H}]$, where $\mathbf{I}_P$ is the identity operator in $\mathcal{H}_P$ space. In this case, the time-dependent translation operator $\hat{S}(t)$ is given by Eq. (4) with the hopping length $J(t)$ at any t, drawn from a Poisson distribution (PD) of different mean values λ, i.e., $\frac{\lambda^b e^{-\lambda}}{b!}$, with b being the event count in PD [38]. Therefore, in this case, $|\psi(t)\rangle = \hat{S}(t) \cdot [I_P \otimes \hat{H}]|\psi(t-1)\rangle$. Additionally, we generate an array of time-dependent random $J(t)$ values for the numerical simulation, with the array length equal to the maximum time steps considered in the CQW dynamics (say, $t = 15$). It represents one disorder realization and, subsequently, the realization average is computed with 500 such realizations for estimating the quantity $\Omega_5(t)$ such as entanglement entropy $E_{\rm av}$ or $P_{\rm av}(x = 0)$, which is defined as $\langle\Omega_5(t)\rangle = \frac{1}{500}\sum_{j=1}^{500} \Omega_5(|\psi(t)\rangle_j\langle\psi(t)|_j)$.

As the hopping (jump) length is a random number, the position disorder violates odd-even parity, which was obeyed in clean CQWs and also in coin and phase disordered CQW,

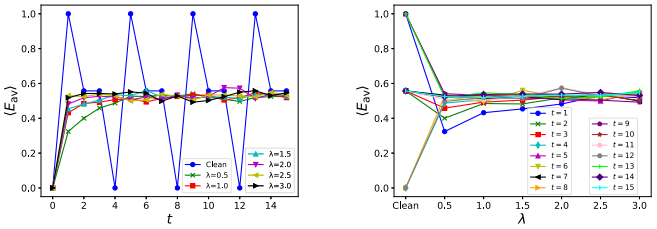

FIG. 4. (a) SPE $\langle E_{\rm av}\rangle$ vs time step t for different position-disorder strength (λ); (b) SPE $\langle E_{\rm av}\rangle$ vs position-disorder strength λ for different t for four cycle.

see Fig. 2 in the SM [35]. We observe that $\langle P_{\rm av}(x=0)\rangle \neq 0$ at odd t, confirming the violation of the odd-even parity for four-cycle CQW evolution. It begets a rich class of superposed and entangled quantum states with finite probabilities of finding the particle at most sites. It helps design cryptographic keys [4,7], as a highly probabilistic (noninferable) public key correlates with greater security in a quantum cryptographic algorithm than a deterministic public key [4,7,39]. Furthermore, the position disorder breaks the physical time cone of the walker and thus can enhance the particle spreading, which helps design search algorithms and study transport phenomena [40–43].

However, SPE is more vulnerable to position disorder than phase or coin disorder. The recurrence or periodicity of the SPE (or MESPS of clean CQW) in four-cycle CQW is distorted under position disorder; see Fig. 4 above, and the SM [35]. Moreover, under position disorder, SPE saturates to a fixed value in both four cycle and three cycle, irrespective of the disorder strength λ, at large t; see Fig. 4 and Sec. D in the SM [35] (Fig. 10). Interestingly, in line with other disorders, a position disorder can also revive SPE at time steps where no SPE was generated via the clean CQW with any arbitrary initial state (see Fig. 4 above).

Analysis. The effects of phase, coin, and position disorder on CQW evolution and SPE are juxtaposed in Table. I. MESPS at $t = 1$ is robust against phase disorder (static and dynamic) of arbitrary strength irrespective of the choice of the initial state. On the other hand, against coin disorder (static and dynamic) of arbitrary strength, MESPS at $t = 1$ is robust for only two phase-symmetric initial states. Also, the reduction in SPE (at any t) is insignificant to low levels of phase and coin disorders (static and dynamic). All disorders are shown to revive SPE from zero and enhance SPE at specific time steps. Unlike coin and phase disorders, position disorder causes SPE to converge to a fixed value at large t (irrespective of the disorder strength and initial state choice). An algorithm to see the effects of disorders via our CQW setup on SPE is provided in Sec. E in the SM [35].

We have also compared our results with prior works, see Refs. [26,27,37,40,44] on DTQW with 1D line in Table I and Sec. F in the SM [35]. References [26,27,37,40,44] focus on generating SPE using disorder (these works considered either a coin or phase or position disorder) and that too for some particular initial states. These proposals do not look at the effects of a disorder on MESPS or SPE (via clean QW). We bridge this gap and comprehensively report on generating SPE via disorder. We also discuss the effects of various disorders on SPE's enhancement, revival, and resilience under phase, coin, and position disorder of arbitrary strength with a most general initial state.

This proposal can be experimentally realized using single photons with optical elements (e.g., polarizing beam splitters, waveplates, Jones plates), wherein the photon's polarization encodes the coin state and time bins or orbital angular momentum encodes the position state [17,18,45–47].

Conclusion and outlook. This study explores the robustness, possibility of revival, and vulnerability of single-particle entanglement (SPE) under phase, coin, and position disorder. Disorders destroy the recurrence of SPE in CQW. The resilience of SPE to minor disorders, particularly phase and coin disorder, demonstrates its potential for stable large-scale QI processing. Phase disorder, especially, leaves maximal SPE (MESPS) states (at $t = 1$) completely unperturbed for any disorder strength, irrespective of the choice of the initial state, i.e., for any arbitrary θ in Eq. (1). Further, phase-symmetric

TABLE I. Disorder effects on SPE in CQW.

	Static		Dynamic		
Property↓ / Disorder→	Phase	Coin	Phase	Coin	Position
Robust MESPS (Bell state) at $t = 1$ to disorder	Yes, for all initial states and disorder strengths [see Eqs. (8) and (9)]	Yes, for phase symmetric initial states and all disorder strengths [see SM [35] Eqs. (12)–(16)]	Yes, for all initial states and disorder strengths [see SM [35] Eq. (7)]	Yes, for phase symmetric initial states and all disorder strengths [see SM [35] Eqs. (17)–(19)]	No
Resilience of SPE to small disorder	Yes	Yes	Yes	Yes	No
Revival of SPE from zero	Yes	Yes	Yes	Yes	Yes
Enhancement of SPE	Yes	Yes	Yes	Yes	Yes
Convergence of SPE to a fixed value	No	No	No	No	Yes, for large disorder strengths

initial states are entirely immune to coin disorder of arbitrary strength. Moreover, phase and coin disorder enhances SPE at specific time steps. These also revive SPE from zero, i.e., from an otherwise separable state, irrespective of the choice of the initial state.

However, unlike coin or phase disorder, position disorder is more deleterious, breaking the odd-even parity and distorting the walker's physical time cone. Position disorder thus generates rich quantum states, which are helpful in quantum cryptography in designing cryptographic keys, as these states will be more challenging to decipher by eavesdroppers as compared to trivial states (product or symmetrically superposed states) [4,7,39]. Besides, position disorder can enhance particle dispersion, increase position standard deviation, and be a resource for an efficient quantum search algorithm and in analyzing transport phenomena [40–43]. Interestingly, despite its disruptive nature, position disorder causes SPE to converge to a fixed value at large t, indicating a level of robustness of SPE even under significant disturbances. These findings underline the nuanced role disorder plays in the evolution of SPE, offering valuable insights for optimizing quantum communication, dynamics of intricate quantum systems in a laboratory setting, and cryptographic protocols that leverage single-particle entangled states.

Data availability. The data that support the findings of this article are openly available [48].

[1] C. Monroe, D. M. Meekhof, B. E. King, and D. J. Wineland, A "Schrödinger Cat" superposition state of an atom, Science **272**, 1131 (1996).

[2] S. Azzini, S. Mazzucchi, V. Moretti, D. Pastorello, and L. Pavesi, Single-particle entanglement, Adv. Quantum Technol. **3**, 2000014 (2020).

[3] X.-X. Fang, Kui An, B.-T. Zhang, B. C. Sanders, and H. Lu, Maximal coin-position entanglement generation in a quantum walk for the third step and beyond regardless of the initial state, Phys. Rev. A **107**, 012433 (2023).

[4] D. K. Panda and C. Benjamin, Recurrent generation of maximally entangled single-particle states via quantum walks on cyclic graphs, Phys. Rev. A **108**, L020401 (2023).

[5] A. Gratsea, M. Lewenstein, and A. Dauphin, Generation of hybrid maximally entangled states in a one-dimensional quantum walk, Quantum Sci. Technol. **5**, 025002 (2020).

[6] C. Vitelli, N. Spagnolo, L. Aparo, F. Sciarrino, E. Santamato, and L. Marrucci, Joining the quantum state of two photons into one, Nat. Photonics **7**, 521 (2013).

[7] D. K. Panda and C. Benjamin, Quantum cryptographic protocols with dual messaging system via 2D alternate quantum walk of a genuine single-photon entangled state, J. Phys. A: Math. Theor. **58**, 01LT01 (2025).

[8] R. Raussendorf and H. J. Briegel, A one-way quantum computer, Phys. Rev. Lett. **86**, 5188 (2001).

[9] M. Blasone, F. Dell'Anno, S. De Siena, M. Di Mauro, and F. Illuminati, Multipartite entangled states in particle mixing, Phys. Rev. D **77**, 096002 (2008).

[10] A. K. Jha, S. Mukherjee, and B. A. Bambah, Tri-partite entanglement in neutrino oscillations, Mod. Phys. Lett. A **36**, 2150056 (2021).

[11] K. H. Kagalwala, G. Di Giuseppe, A. F. Abouraddy, and B. E. A. Saleh, Single-photon three-qubit quantum logic using spatial light modulators, Nat. Commun. **8**, 739 (2017).

[12] P. Imany, N. B. Lingaraju, M. S. Alshaykh, D. E. Leaird, and A. M. Weiner, Probing quantum walks through coherent control of high-dimensionally entangled photons, Sci. Adv. **6**, eaba8066 (2020).

[13] D. K. Panda, B. V. Govind, and C. Benjamin, Generating highly entangled states via discrete-time quantum walks with Parrondo sequences, Physica A **608**, 128256 (2022).

[14] Y. Aharonov, L. Davidovich, and N. Zagury, Quantum random walks, Phys. Rev. A **48**, 1687 (1993).

[15] D. K. Panda and C. Benjamin, Designing three-way-entangled and nonlocal two-way-entangled single-particle states via alternate quantum walks, Phys. Rev. A **111**, 012420 (2025).

[16] H. B. Perets *et al.*, Realization of quantum walks with negligible decoherence in waveguide lattices, Phys. Rev. Lett. **100**, 170506 (2008).

[17] M. Karski *et al.*, Quantum walk in position space with single optically trapped atoms, Science **325**, 174 (2009).

[18] Z.-H. Bian, J. Li, X. Zhan, J. Twamley, and P. Xue, Experimental implementation of a quantum walk on a circle with single photons, Phys. Rev. A **95**, 052338 (2017).

[19] A. Peruzzo *et al.*, Quantum walks of correlated photons, Science **329**, 1500 (2010).

[20] A. Schreiber *et al.*, Photons walking the line: A quantum walk with adjustable coin operations, Phys. Rev. Lett. **104**, 050502 (2010).

[21] M. A. Broome *et al.*, Discrete single-photon quantum walks with tunable decoherence, Phys. Rev. Lett. **104**, 153602 (2010).

[22] M. Tamura, T. Mukaiyama, and K. Toyoda, Quantum walks of a phonon in trapped ions, Phys. Rev. Lett. **124**, 200501 (2020).

[23] H. Schmitz *et al.*, Quantum walk of a trapped ion in phase space, Phys. Rev. Lett. **103**, 090504 (2009).

[24] F. Zähringer *et al.*, Realization of a quantum walk with one and two trapped ions, Phys. Rev. Lett. **104**, 100503 (2010).

[25] C. A. Ryan, M. Laforest, J. C. Boileau, and R. Laflamme, Experimental implementation of a discrete-time quantum random walk on an NMR quantum-information processor, Phys. Rev. A **72**, 062317 (2005).

[26] L. H. Yao and S. Wald, Coined quantum walks on the line: Disorder, entanglement, and localization, Phys. Rev. E **108**, 024139 (2023).

[27] R. Vieira, E. P. M. Amorim, and G. Rigolin, Dynamically disordered quantum walk as a maximal entanglement generator, Phys. Rev. Lett. **111**, 180503 (2013).

[28] J. Marino and S. Diehl, Driven Markovian quantum criticality, Phys. Rev. Lett. **116**, 070407 (2016).

[29] K. Seetharam, A. Lerose, R. Fazio, and J. Marino, Correlation engineering via nonlocal dissipation, Phys. Rev. Res. **4**, 013089 (2022).

[30] F. Verstraete, M. M. Wolf, and J. Ignacio Cirac, Quantum computation and quantum-state engineering driven by dissipation, Nat. Phys. **5**, 633 (2009).

[31] C. Muzzi, M. Tsitsishvili, and G. Chiriacò, Entanglement enhancement induced by noise in inhomogeneously monitored systems, Phys. Rev. B **111**, 014312 (2025).
[32] Z. Cai, R. Babbush, S. C. Benjamin, S. Endo, W. J. Huggins, Y. Li, J. R. McClean, and T. E. O'Brien, Quantum error mitigation, Rev. Mod. Phys. **95**, 045005 (2023).
[33] A. Lowe, M. H. Gordon, P. Czarnik, A. Arrasmith, P. J. Coles, and L. Cincio, Unified approach to data-driven quantum error mitigation, Phys. Rev. Res. **3**, 033098 (2021).
[34] A. Kandala, K. Temme, A. D. Córcoles, A. Mezzacapo, J. M. Chow, and J. M. Gambetta, Error mitigation extends the computational reach of a noisy quantum processor, Nature (London) **567**, 491 (2019).
[35] See Supplemental Material at http://link.aps.org/supplemental/10.1103/PhysRevE.111.L042103 for more details, which includes Refs. [4,7,26,27,37,40–44].
[36] D. Janzing, *Entropy of Entanglement*, Compendium of Quantum Physics (Springer, Berlin, Heidelberg, 2009), pp. 205–209.
[37] M. Zeng and E. H. Yong, Discrete-time quantum walk with phase disorder: Localization and entanglement entropy, Sci. Rep. **7**, 12024 (2017).
[38] S. Das, S. Mal, A. Sen(De), and U. Sen, Inhibition of spreading in quantum random walks due to quenched Poisson-distributed disorder, Phys. Rev. A **99**, 042329 (2019).
[39] D. J. Bernstein and T. Lange, Post-quantum cryptography, Nature (London) **549**, 188 (2017).
[40] C. B. Naves, M. A. Pires, D. O. Soares-Pinto, and S. M. Duarte Queirós, Enhancing entanglement with the generalized elephant quantum walk from localized and delocalized states, Phys. Rev. A **106**, 042408 (2022).
[41] M. A. Pires, G. Di Molfetta, and S. M. D. Queirós, Multiple transitions between normal and hyperballistic diffusion in quantum walks with time-dependent jumps, Sci. Rep. **9**, 19292 (2019).
[42] G. Di Molfetta, D. O. Soares-Pinto, and S. M. D. Queirós, Elephant quantum walk, Phys. Rev. A **97**, 062112 (2018).
[43] R. Portugal, *Quantum Walks and Search Algorithms* (Springer, New York, 2013).
[44] T.-T. Liu *et al.*, The entanglement of deterministic aperiodic quantum walks, Chinese Phys. B **27**, 120305 (2018).
[45] P. A. A. Yasir and C. M. Chandrashekar, Generation of hyperentangled states and two-dimensional quantum walks using J or q plates and polarization beam splitters, Phys. Rev. A **105**, 012417 (2022).
[46] R. C. Devlin, A. Ambrosio, N. A. Rubin, J. P. B. Mueller, and F. Capasso, Arbitrary spin-to–orbital angular momentum conversion of light, Science **358**, 896 (2017).
[47] H. Tang *et al.*, Experimental two-dimensional quantum walk on a photonic chip, Sci. Adv. **4**, eaat3174 (2018).
[48] D. K. Panda and C. Benjamin, The Python codes used to generate the numerical results and plots in the study are available in the public repository GitHub, see https://github.com/Quantum-Panda97/PyCode-disorder-effect-on-entanglement (2025).